

# Zero shot framework for satellite image restoration

Praveen Kandula, and A. N. Rajagopalan, *Senior Member, IEEE*

**Abstract**—Satellite images are typically subject to multiple distortions. Different factors affect the quality of satellite images, including changes in atmosphere, surface reflectance, sun illumination, viewing geometries etc., limiting its application to downstream tasks. In supervised networks, the availability of paired datasets is a strong assumption. Consequently, many unsupervised algorithms have been proposed to address this problem. These methods synthetically generate a large dataset of degraded images using image formation models. A neural network is then trained with an adversarial loss to discriminate between images from distorted and clean domains. However, these methods yield suboptimal performance when tested on real images that do not necessarily conform to the generation mechanism. Also, they require a large amount of training data and are rendered unsuitable when only a few images are available. We propose a distortion disentanglement and knowledge distillation framework for satellite image restoration to address these important issues. Our algorithm requires only two images: the distorted satellite image to be restored and a reference image with similar semantics. Specifically, we first propose a mechanism to disentangle distortion. This enables us to generate images with varying degrees of distortion using the disentangled distortion and the reference image. We then propose the use of knowledge distillation to train a restoration network using the generated image pairs. As a final step, the distorted image is passed through the restoration network to get the final output. Ablation studies show that our proposed mechanism successfully disentangles distortion. Exhaustive experiments on different timestamps of Google-Earth images and publicly available datasets, LEVIR-CD and SZTAKI, show that our proposed mechanism can tackle a variety of distortions and outperforms existing state-of-the-art restoration methods visually as well as on quantitative metrics.

## I. INTRODUCTION AND RELATED WORKS

Satellite imagery is used for different applications, including extracting mineral deposits, agriculture development, disaster mitigation, weather forecast etc. Unfortunately, the quality of the captured images is affected by intrinsic properties of acquisition systems, and imaging conditions. While the intrinsic properties include physical condition of sensors, detectors, camera tilts etc., the quality of satellite images is also affected by terrain, atmospheric bending, sun illumination, and viewing angles during the time of capture. The combined effect of these distortions (or degradations) is difficult to model mathematically, rendering the existing satellite restoration works [1]–[9] unsuitable for real-world images. We use the words ‘distortions’ and ‘degradations’ interchangeably in this paper.

Learning-based deep networks give impressive results for individual restoration tasks like deblurring [10]–[25], dehazing [26]–[29], inpainting [30], [31], enhancement [32], [33], super-resolution [34]–[40], bokeh rendering [41], inpainting [31], [42] etc. Unsupervised methods relax the need for paired datasets for training a deep net. In this setting, a large dataset of clean and distorted images is required without the need to enforce the criterion of paired images. These methods typically

have CycleGAN [43] as a backbone and discriminate images from clean and distorted domains using cycle consistency and adversarial losses. This formulation has been successfully employed for different restoration tasks like denoising [44], [45], super-resolution [46], shadow-removal [47], etc., with suitable modifications in loss functions and network architecture. Although paired images are not required, pooling a large number of distorted images remains a challenge. To tackle this, unsupervised methods resort to synthesizing distortions using different formulations akin to supervised techniques.

In this paper, we propose a learning-based algorithm to restore a distorted satellite image using a reference image. We propose a distortion disentanglement and knowledge distillation mechanism for image restoration, which addresses the shortcomings of previous works. Although our method requires a reference image, this is not difficult to acquire in satellite imaging, where images are taken at regular intervals. The captured image might have undesirable artifacts due to low light, weather conditions etc., but there is a high probability that at least one past image is distortion-free. Using reference image as input, recent supervised super-resolution networks [48], [49] showed improved performance. Our algorithm can be considered as an extension of existing zero-shot and reference-based algorithms. Different from zero-shot methods, our method uses a reference image in addition to an input image during training.

The main contributions of our work are summarized below:

- To the best of our knowledge, this is the first-ever learning-based approach to explicitly separate distortion information from a degraded satellite image using only a pair of images (distorted and reference images).
- We propose feature adversarial loss and feature regularization loss to train distortion disentanglement network (DDN). Different ablation studies show that our design architecture and loss functions in DDN effectively decouple content and distortion from an input image.
- A unique strength of our method is that it is not distortion-specific i.e., the proposed algorithm restores satellite images with unknown and challenging distortions. Also, our algorithm does not warrant the reference and distorted images to be exactly aligned.

## II. PROPOSED METHOD

The objective of our method is to restore a distorted satellite image  $I_d$  using a clean reference image  $I_r$ . For conciseness, the distorted satellite image is referred to as distorted image. Also, the content in  $I_r$  is not required to perfectly match that of  $I_d$ , i.e.,  $I_r$  and  $I_d$  can be captured at different time stamps.

Since these images share similar scene semantics, one possible approach is to use supervised networks with  $I_r$  and

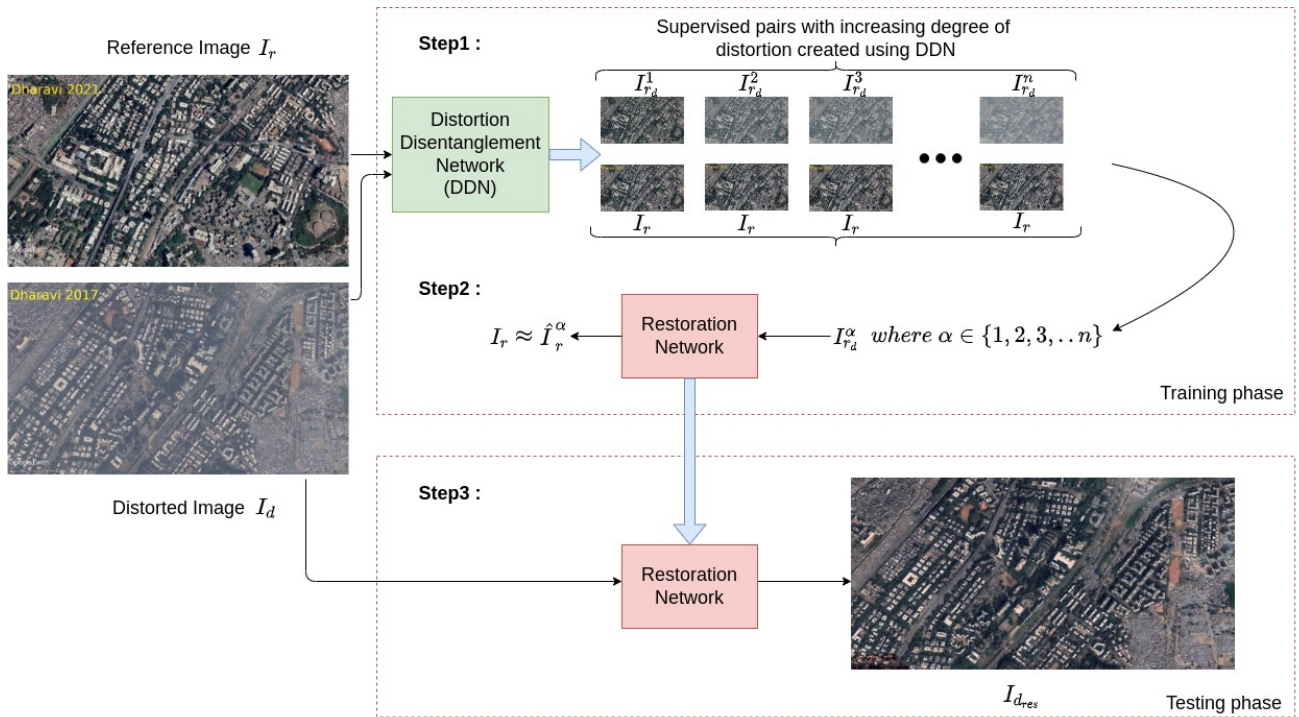


Fig. 1. Proposed network architecture. Given a reference image ( $I_r$ ) and distorted image ( $I_d$ ), the objective is to restore  $I_d$  using  $I_r$ . Here,  $I_r$  and  $I_d$  are real satellite images from 2017 and 2021, respectively, from Dharavi (Mumbai). The proposed restoration mechanism involves three steps. In step1, a distortion disentanglement network (DDN) is used to decouple the content and distortion information from  $I_d$ . Supervised pairs with increasing degrees of distortion are created using decoupled information. In the second step, a restoration network is trained using the supervised pairs. As the last step, the distorted image ( $I_d$ ) is passed through the trained restoration network for the final restored image ( $I_{d_{res}}$ ). A major highlight of our algorithm is that the proposed model needs only a pair of images ( $I_r$  and  $I_d$ ) for restoration. Also, a unique strength of our algorithm is that it is not distortion specific i.e., since the DDN couples distortion from input images, our model can handle challenging and unknown distortions.

$I_d$  as paired images over pixel-wise loss functions. However, the restored image is noisy and lacks structural coherence (see Fig. 3, third row). This can be attributed to two reasons. First, although  $I_r$  and  $I_d$  share scene semantics, they are not necessarily aligned. For instance, the aircrafts in  $I_r$  is geometrically off by a significant margin compared to  $I_d$ . These misalignments can badly affect the outcome for supervised loss functions. In addition, since  $I_d$  and  $I_r$  are imaged at different timestamps, there can be significant differences in their image contents. Nonetheless, supervised loss functions fit the non-existent information in the distorted image to the one present in reference images resulting in bad test results.

#### A. Disentanglement of distortion

Given a reference image ( $I_r$ ) and distorted image ( $I_d$ ), the objective is to disentangle distortion information from  $I_d$  using  $I_r$ . This is a challenging task as we are provided with only two images. DDN has three sub networks, a content encoder  $E_c$ , a distortion encoder  $E_d$ , and a decoder  $D$ . Given the distorted image  $I_d$ ,  $E_c$  extracts only content information, while  $E_d$  extracts only distortion information. Since  $I_r$  does not contain any distortion information,  $E_d$  does not extract any information from it. Given  $I_d$  (or  $I_r$ ),  $D$  uses the combined feature maps of  $E_c$  and  $E_d$  to estimate the corresponding image. To ensure that  $E_c$  extracts only content information from the given image, we adopt the following strategy.

- Since  $I_r$  is free from distortion,  $E_c$  must ideally extract only content information. Let the output of  $E_c$  given  $I_r$  be denoted as  $F_{r_c} \in R^{1 \times C \times H \times W}$ , where  $C, H, W$  are number of channels, height and width of feature map  $F_{r_c}$ , respectively.
- Given  $I_d$ ,  $E_c$  should extract only content features. Let the output of  $E_c$  given  $I_d$  be denoted as  $F_{d_c} \in R^{1 \times C \times H \times W}$ , where  $C, H, W$  are as mentioned above. In order to ensure that  $E_c$  extracts only content information, we propose to use adversarial loss on feature maps. The feature maps  $F_{r_c}$  are used as real samples while  $F_{d_c}$  are the fake samples. The loss function for this objective is termed feature adversarial loss and is formulated as

$$\mathbb{L}_{adv}(E_c, E_d, D, D_{adv}) = \mathbb{E}[\log(D_{adv}(F_{r_c}))] + \mathbb{E}[\log(1 - D_{adv}(F_{d_c}))] \quad (1)$$

#### B. Feature regularization loss

The motivation for this loss function is to ensure that  $E_d$  does not respond to  $I_r$ , since  $I_r$  is distortionless. We achieve this by constraining all the output feature maps of  $E_d$  to zero. This also ensures that  $E_d$  extracts only distortion information from  $I_d$ . This loss function is formulated as

$$L_{reg} = \left\| \sum_{i=1}^{\rho} F_{r_d}^i \right\|_1 \quad (2)$$

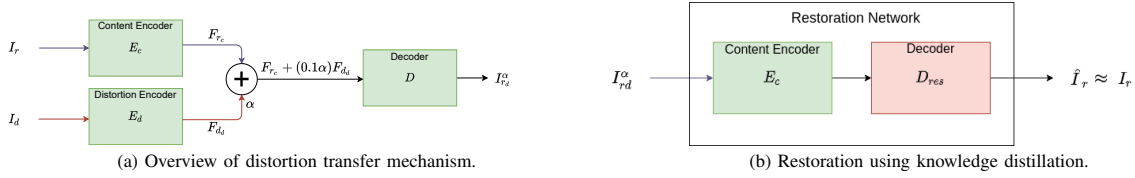


Fig. 2. (a) Given  $I_r$  and  $I_d$ , the objective is to transfer distortion from  $I_d$  to  $I_r$ . To achieve this, feature maps of  $E_c$  given  $I_r$  ( $F_{r_c}$ ) is combined with feature maps of  $E_d$  given  $I_d$  ( $F_{d_d}$ ) and passed through the decoder network. A detailed explanation of the distortion transfer mechanism is given in Sec. II-D. (b) Instead of using a vanilla encoder-decoder network for training restoration network,  $E_c$  from distortion disentanglement network (DDN) is used as encoder network, which improves the convergence rate.

where  $F_{r_d}^i$  is the output feature map of  $E_d$  with  $I_r$  as input and  $i$  denotes intermediate feature maps of  $E_d$ .

### C. Cyclic loss functions

In order to ensure that the Decoder  $D$  is effectively trained to recover the input image, we use cyclic loss functions on  $I_r$  and  $I_d$ . Given  $I_d$ ,  $E_c$  encodes only content information while  $E_d$  encodes only distortion due to  $L_{adv}$  and  $L_{reg}$ .  $D$  takes combined feature maps of  $E_c$  and  $E_d$  to get back the input image  $I_d$ . The cyclic loss function for  $I_d$  can be defined as

$$L_{d_{cy}} = \|D(E_c(I_d) + E_d(I_d)) - I_d\|_1 \quad (3)$$

Similarly, cyclic loss for  $I_r$  is defined as

$$L_{r_{cy}} = \|D(E_c(I_r) + E_d(I_r)) - I_r\|_1 \quad (4)$$

where  $L_{d_{cy}}$  and  $L_{r_{cy}}$  refer to distortion cyclic loss and reference cyclic loss functions, respectively. While  $L_{adv}$  and  $L_{reg}$  ensure that  $E_c$  extracts only content information, the cyclic losses  $L_{d_{cy}}$  and  $L_{r_{cy}}$  force  $E_d$  to learn distortion information from input images in addition to estimating the corresponding input image.

The total loss function used in our disentanglement framework is the combination of the above loss functions. All the loss functions are used within a single iteration, and the four networks ( $E_c$ ,  $E_d$ ,  $D$ ,  $D_{adv}$ ) are trained end-to-end. The final loss function for our distortion disentanglement network methodology can be written as

$$L_{Total} = \lambda_1 L_{adv} + \lambda_2 L_{reg} + \lambda_3 L_{d_{cy}} + \lambda_4 L_{r_{cy}} \quad (5)$$

where  $\lambda_1$ ,  $\lambda_2$ ,  $\lambda_3$ , and  $\lambda_4$  refer to trade-off weights balancing different loss functions.

### D. Distortion transfer

Once the DDN is trained using  $L_{Total}$ , the modules  $E_c$  and  $E_d$  extract only content and distortion information, respectively, from any input image. To transfer the distortion from  $I_d$  to  $I_r$ , we use the distortion transfer mechanism illustrated in Fig. 2 (a) and formulated as

$$I_{r_d}^{\alpha} = D(F_{r_c} + (0.1\alpha)F_{d_d}) \quad (6)$$

where  $F_{r_c}$  represents the output feature maps of  $E_c$  given  $I_r$ ,  $F_{d_d}$  the output feature maps of  $E_d$  for  $I_d$  image,  $I_{r_d}^{\alpha}$  is the result of the distortion transfer mechanism and  $\alpha \in 1, 2, \dots, n$ . The objective of  $\alpha$  is to create varying degrees of distortion on  $I_r$ . Using this mechanism, a dataset of supervised pairs,  $(I_{r_d}^1, I_r), (I_{r_d}^2, I_r), \dots, (I_{r_d}^n, I_r)$  is created. The key idea behind using different values of  $\alpha$  is to train a robust restoration network that can effectively restore  $I_d$ .

### E. Restoration by knowledge distillation

We propose to use the supervised pairs (created by distortion transfer) within a knowledge distillation (KD) framework to restore  $I_d$  effectively. Inspired by acceleration techniques [50] (a type of KD) that transfer the convolutional filters from one model to another, we take advantage of the information learned during the disentanglement process. Specifically, we use an encoder-decoder model for restoration, with encoder being the pretrained network  $E_c$  (from DDN) that can judiciously extract content features from input images. We fix the encoder model and update the parameters of the decoder ( $D_{res}$ ) alone using MSE loss as shown in Fig. 2 (b). This can be formulated as

$$\hat{I}_r^{\alpha} = D_{res}(E_c(I_{r_d}^{\alpha})) \quad (7)$$

where  $\hat{I}_r^{\alpha}$  is the output of the restoration network given  $I_{r_d}^{\alpha}$ . The main advantage of using a KD mechanism is that the restoration network can be accelerated and efficiently trained. The convergence time using the proposed mechanism is significantly reduced compared to a network that trains from scratch.

Note that DDN disentangles distortion in  $I_d$ , while the restoration network is efficiently trained to tackle that distortion. The restoration network is trained robustly by varying  $\alpha$  in Eq. 6 to effectively handle different amounts of distortion. As a final step,  $I_d$  is passed through the trained restoration network to obtain the output restored image, as shown in Fig. 1. This can be written as

$$I_{d_{res}} = D_{res}(E_c(I_d)) \quad (8)$$

where  $I_{d_{res}}$  is the final restored output given  $I_d$  as input to the restoration network.

## III. EXPERIMENTS

The experiments section is arranged as follows: (i) implementation details, (ii) dataset and competing methods, (iii) ablation studies, (iv) metrics used, quantitative comparisons, and (v) visual comparisons.

### A. Implementation details

We use Pytorch library to train both DDN and restoration networks. We first train DDN using Eq. 5 with weights for different loss functions set as  $\lambda_1=1$ ,  $\lambda_2=10$ ,  $\lambda_3=1$  and  $\lambda_4=1$ . Then a supervised dataset with varying amounts of distortion is created from the distortion transfer mechanism using Eq. 6 with  $n=100$ , i.e., hundred distorted images are

created to train the restoration network. The DDN network is trained for 4000 iterations, while the restoration network is trained for 150 epochs. For both DDN and restoration network, we use the following options: ADAM optimizer to update the model parameters, momentum values with  $\beta_1 = 0.9$  and  $\beta_2 = 0.99$ , patch size of 512 (original size of all the images is 1280x780) and a learning rate of 0.0001. Inference and convergence times for DDN and restoration network are discussed in supplementary. VGGSR [51] showed that the features extracted from initial layers of VGG16 [52] can be used for different downstream tasks such as denoising and super-resolution.

We mainly compare our method with unsupervised methods CycleGAN [43], DCLGAN [53], UDSD [54], UEGAN [55] and two supervised restoration methods DHMP [56], and VGGSR [51]. Additionally, we evaluated the performance of our model on two publicly available datasets, LEVIR-CD [57], and SZTAKI [58].

#### IV. CONCLUSION

We proposed a deep learning framework for restoring a distorted satellite image using a reference image. We showed that content and distortion present in the image can be effectively decoupled. This allowed us to transfer the distortion to a clean image and create distortion-clean image pairs. With these supervised pairs, a restoration network was efficiently trained using knowledge distillation. Extensive ablation studies were conducted to reveal the effect of the loss functions used in our network. The performance of our method is superior to prior art both visually and on standard image quality assessment metrics. The restoration results reveal that our algorithm can successfully handle images suffering from multiple distortions.

#### REFERENCES

- [1] H. M. Keshk and X.-C. Yin, "Satellite super-resolution images depending on deep learning methods: a comparative study," in *2017 IEEE International Conference on Signal Processing, Communications and Computing (ICSPCC)*. IEEE, 2017, pp. 1–7. 1
- [2] P. Gupta and R. Mehra, "Blind restoration method for satellite images using memetic algorithm," *International Journal of Computer Applications*, vol. 975, p. 8887, 2015. 1
- [3] G. Bi, G. Si, Y. Zhao, B. Qi, and H. Lv, "Haze removal for a single remote sensing image using low-rank and sparse prior," *IEEE Transactions on Geoscience and Remote Sensing*, vol. 60, pp. 1–13, 2021. 1
- [4] Y. Qian, H. Zhu, L. Chen, and J. Zhou, "Hyperspectral image restoration with self-supervised learning: A two-stage training approach," *IEEE Transactions on Geoscience and Remote Sensing*, vol. 60, pp. 1–17, 2021. 1
- [5] X. Yang, X. Wang, N. Wang, and X. Gao, "Srdn: A unified super-resolution and motion deblurring network for space image restoration," *IEEE Transactions on Geoscience and Remote Sensing*, vol. 60, pp. 1–11, 2021. 1
- [6] M. Shao, C. Wang, W. Zuo, and D. Meng, "Efficient pyramidal gan for versatile missing data reconstruction in remote sensing images," *IEEE Transactions on Geoscience and Remote Sensing*, 2022. 1
- [7] A. Mohan, R. Dwivedi, and B. Kumar, "Image restoration of landslide photographs using srcnn," *Recent Trends in Electronics and Communication*, pp. 1249–1259, 2022. 1
- [8] H. Jiang, M. Peng, Y. Zhong, H. Xie, Z. Hao, J. Lin, X. Ma, and X. Hu, "A survey on deep learning-based change detection from high-resolution remote sensing images," *Remote Sensing*, vol. 14, no. 7, p. 1552, 2022. 1
- [9] S. Jiang, X. Zhi, T. Shi, J. Hu, W. Zhang, and J. Gong, "Influence of space variability on remote sensing image restoration performances," *IEEE Geoscience and Remote Sensing Letters*, 2022. 1
- [10] S. Vasu, V. R. Maligireddy, and A. Rajagopalan, "Non-blind deblurring: Handling kernel uncertainty with cnns," in *Proceedings of the IEEE Conference on Computer Vision and Pattern Recognition*, 2018, pp. 3272–3281. 1
- [11] M. M. Mohan, G. Nithin, and A. Rajagopalan, "Deep dynamic scene deblurring for unconstrained dual-lens cameras," *IEEE Transactions on Image Processing*, vol. 30, pp. 4479–4491, 2021. 1
- [12] T. M. Nimisha, K. Sunil, and A. Rajagopalan, "Unsupervised class-specific deblurring," in *Proceedings of the European Conference on Computer Vision (ECCV)*, 2018, pp. 353–369. 1
- [13] M. P. Rao, A. Rajagopalan, and G. Seetharaman, "Harnessing motion blur to unveil splicing," *IEEE transactions on information forensics and security*, vol. 9, no. 4, pp. 583–595, 2014. 1
- [14] A. N. Rajagopalan and S. Chaudhuri, "Optimal recovery of depth from defocused images using an mrf model," in *Sixth International Conference on Computer Vision (IEEE Cat. No. 98CH36271)*. IEEE, 1998, pp. 1047–1052. 1
- [15] C. Paramanand and A. N. Rajagopalan, "Depth from motion and optical blur with an unscented kalman filter," *IEEE Transactions on Image Processing*, vol. 21, no. 5, pp. 2798–2811, 2011. 1
- [16] K. Purohit and A. Rajagopalan, "Region-adaptive dense network for efficient motion deblurring," in *Proceedings of the AAAI Conference on Artificial Intelligence*, vol. 34, no. 07, 2020, pp. 11 882–11 889. 1
- [17] S. Vasu and A. Rajagopalan, "From local to global: Edge profiles to camera motion in blurred images," in *Proceedings of the IEEE Conference on Computer Vision and Pattern Recognition*, 2017, pp. 4447–4456. 1
- [18] T. Nimisha, A. Rajagopalan, and R. Aravind, "Generating high quality pan-shots from motion blurred videos," *Computer Vision and Image Understanding*, vol. 171, pp. 20–33, 2018. 1
- [19] M. Suin, K. Purohit, and A. Rajagopalan, "Spatially-attentive patch-hierarchical network for adaptive motion deblurring," in *Proceedings of the IEEE/CVF Conference on Computer Vision and Pattern Recognition*, 2020, pp. 3606–3615. 1
- [20] K. Purohit, A. Shah, and A. Rajagopalan, "Bringing alive blurred moments," in *Proceedings of the IEEE/CVF Conference on Computer Vision and Pattern Recognition*, 2019, pp. 6830–6839. 1
- [21] M. Mohan, S. Girish, and A. Rajagopalan, "Unconstrained motion deblurring for dual-lens cameras," in *Proceedings of the IEEE/CVF International Conference on Computer Vision*, 2019, pp. 7870–7879. 1
- [22] K. Purohit and A. Rajagopalan, "Efficient motion deblurring with feature transformation and spatial attention," in *2019 IEEE International Conference on Image Processing (ICIP)*. IEEE, 2019, pp. 4674–4678. 1
- [23] M. Suin and A. Rajagopalan, "Gated spatio-temporal attention-guided video deblurring," in *Proceedings of the IEEE/CVF Conference on Computer Vision and Pattern Recognition*, 2021, pp. 7802–7811. 1
- [24] K. Purohit, S. Vasu, M. P. Rao, and A. Rajagopalan, "Multi-planar geometry and latent image recovery from a single motion-blurred image," *Machine Vision and Applications*, vol. 33, no. 1, p. 10, 2022. 1
- [25] N. Varghese, M. M. MR, and A. Rajagopalan, "Fast motion-deblurring of ir images," *IEEE Signal Processing Letters*, vol. 29, pp. 459–463, 2022. 1
- [26] C. O. Ancuti, C. Ancuti, R. Timofte, L. Van Gool, L. Zhang, and M.-H. Yang, "Ntire 2019 image dehazing challenge report," in *Proceedings of the IEEE/CVF Conference on Computer Vision and Pattern Recognition Workshops*, 2019, pp. 0–0. 1
- [27] K. Purohit, S. Mandal, and A. Rajagopalan, "Multilevel weighted enhancement for underwater image dehazing," *JOSA A*, vol. 36, no. 6, pp. 1098–1108, 2019. 1
- [28] W. Ren, S. Liu, H. Zhang, J. Pan, X. Cao, and M.-H. Yang, "Single image dehazing via multi-scale convolutional neural networks," in *European conference on computer vision*. Springer, 2016, pp. 154–169. 1
- [29] S. Mandal and A. Rajagopalan, "Local proximity for enhanced visibility in haze," *IEEE Transactions on Image Processing*, vol. 29, pp. 2478–2491, 2019. 1
- [30] J. Yu, Z. Lin, J. Yang, X. Shen, X. Lu, and T. S. Huang, "Generative image inpainting with contextual attention," in *Proceedings of the IEEE conference on computer vision and pattern recognition*, 2018, pp. 5505–5514. 1

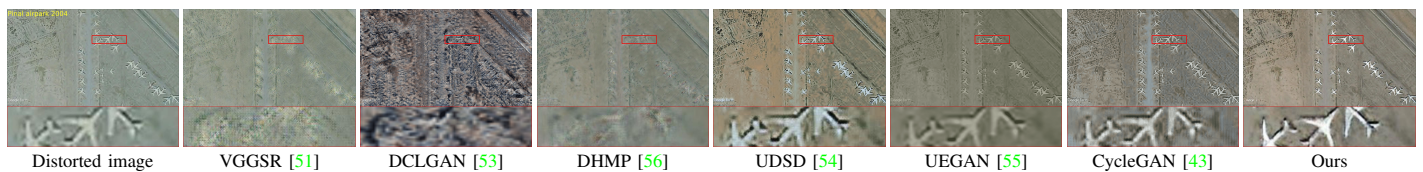


Fig. 3. Visual comparisons with state-of-the-art restoration methods on real satellite images. The distorted image in the top row (1.(a)) suffers from blur artifacts and has green colour tinge all over the image. Similarly, distorted image in third row (2. (a)) also has colour cast and contents are not clearly visible. Competing methods clearly failed to restore the missing details and remove the colour tinge. Even in the CycleGAN (1.(g)), green colour is still present and airplane structure is deformed. On the other hand, results of our method completely removed the unwanted colours and the contents are clearly visible.

- [31] M. Suin, K. Purohit, and A. Rajagopalan, "Distillation-guided image inpainting," in *Proceedings of the IEEE/CVF International Conference on Computer Vision*, 2021, pp. 2481–2490. 1
- [32] P. Kandula, M. Suin, and A. Rajagopalan, "Illumination-adaptive unpaired low-light enhancement," *IEEE Transactions on Circuits and Systems for Video Technology*, 2023. 1
- [33] M. El Helou, R. Zhou, S. Süsstrunk, R. Timofte, M. Afifi, M. S. Brown, K. Xu, H. Cai, Y. Liu, L.-W. Wang *et al.*, "Aim 2020: Scene relighting and illumination estimation challenge," in *Computer Vision—ECCV 2020 Workshops: Glasgow, UK, August 23–28, 2020, Proceedings, Part III 16*. Springer, 2020, pp. 499–518. 1
- [34] M. Suin, K. Purohit, and A. Rajagopalan, "Degradation aware approach to image restoration using knowledge distillation," *IEEE Journal of Selected Topics in Signal Processing*, vol. 15, no. 2, pp. 162–173, 2020. 1
- [35] A. N. Rajagopalan and V. P. Kiran, "Motion-free superresolution and the role of relative blur," *JOSA A*, vol. 20, no. 11, pp. 2022–2032, 2003. 1
- [36] K. Purohit, M. Suin, A. Rajagopalan, and V. N. Boddeti, "Spatially-adaptive image restoration using distortion-guided networks," in *Proceedings of the IEEE/CVF International Conference on Computer Vision*, 2021, pp. 2309–2319. 1
- [37] K. V. Suresh and A. N. Rajagopalan, "Robust and computationally efficient superresolution algorithm," *JOSA A*, vol. 24, no. 4, pp. 984–992, 2007. 1
- [38] A. V. Bhavsar and A. Rajagopalan, "Resolution enhancement in multi-image stereo," *IEEE transactions on pattern analysis and machine intelligence*, vol. 32, no. 9, pp. 1721–1728, 2010. 1
- [39] K. Purohit, S. Mandal, and A. Rajagopalan, "Mixed-dense connection networks for image and video super-resolution," *Neurocomputing*, vol. 398, pp. 360–376, 2020. 1
- [40] T. Nimisha and A. Rajagopalan, "Blind super-resolution of faces for surveillance," *Deep Learning-Based Face Analytics*, pp. 119–136, 2021. 1
- [41] K. Purohit, M. Suin, P. Kandula, and R. Ambasamudram, "Depth-guided dense dynamic filtering network for bokeh effect rendering," in *2019 IEEE/CVF International Conference on Computer Vision Workshop (ICCVW)*. IEEE, 2019, pp. 3417–3426. 1
- [42] A. V. Bhavsar and A. N. Rajagopalan, "Range map superresolution-inpainting, and reconstruction from sparse data," *Computer Vision and Image Understanding*, vol. 116, no. 4, pp. 572–591, 2012. 1
- [43] J.-Y. Zhu, T. Park, P. Isola, and A. A. Efros, "Unpaired image-to-image translation using cycle-consistent adversarial networks," in *Proceedings-1 of the IEEE international conference on computer vision*, 2017, pp. 2223–2232. 1, 4, 5
- [44] J. Xu, Y. Huang, M.-M. Cheng, L. Liu, F. Zhu, Z. Xu, and L. Shao, "Noisy-as-clean: learning self-supervised denoising from corrupted image," *IEEE Transactions on Image Processing*, vol. 29, pp. 9316–9329, 2020. 1
- [45] A. Rajagopalan, R. Chellappa, and N. T. Koterba, "Background learning for robust face recognition with pca in the presence of clutter," *IEEE Transactions on Image Processing*, vol. 14, no. 6, pp. 832–843, 2005. 1
- [46] Y. Yuan, S. Liu, J. Zhang, Y. Zhang, C. Dong, and L. Lin, "Unsupervised image super-resolution using cycle-in-cycle generative adversarial networks," in *Proceedings of the IEEE Conference on Computer Vision and Pattern Recognition Workshops*, 2018, pp. 701–710. 1
- [47] X. Hu, Y. Jiang, C.-W. Fu, and P.-A. Heng, "Mask-shadowgan: Learning to remove shadows from unpaired data," in *Proceedings of the IEEE/CVF International Conference on Computer Vision*, 2019, pp. 2472–2481. 1
- [48] G. Shim, J. Park, and I. S. Kweon, "Robust reference-based super-resolution with similarity-aware deformable convolution," in *Proceedings of the IEEE/CVF Conference on Computer Vision and Pattern Recognition*, 2020, pp. 8425–8434. 1
- [49] Y. Jiang, K. C. Chan, X. Wang, C. C. Loy, and Z. Liu, "Robust reference-based super-resolution via c2-matching," in *Proceedings of the IEEE/CVF Conference on Computer Vision and Pattern Recognition*, 2021, pp. 2103–2112. 1
- [50] J. Gou, B. Yu, S. J. Maybank, and D. Tao, "Knowledge distillation: A survey," *International Journal of Computer Vision*, vol. 129, no. 6, pp. 1789–1819, 2021. 3
- [51] J. Johnson, A. Alahi, and L. Fei-Fei, "Perceptual losses for real-time style transfer and super-resolution," in *European conference on computer vision*. Springer, 2016, pp. 694–711. 4, 5
- [52] K. Simonyan and A. Zisserman, "Very deep convolutional networks for large-scale image recognition," *arXiv preprint arXiv:1409.1556*, 2014. 4
- [53] J. Han, M. Shoeiby, L. Petersson, and M. A. Armin, "Dual contrastive learning for unsupervised image-to-image translation," in *Proceedings of the IEEE/CVF Conference on Computer Vision and Pattern Recognition*, 2021, pp. 746–755. 4, 5
- [54] B. Lu, J.-C. Chen, and R. Chellappa, "Unsupervised domain-specific deblurring via disentangled representations," in *Proceedings of the IEEE/CVF Conference on Computer Vision and Pattern Recognition*, 2019, pp. 10225–10234. 4, 5
- [55] Z. Ni, W. Yang, S. Wang, L. Ma, and S. Kwong, "Towards unsupervised deep image enhancement with generative adversarial network," *IEEE Transactions on Image Processing*, vol. 29, pp. 9140–9151, 2020. 4, 5
- [56] H. Zhang, Y. Dai, H. Li, and P. Koniusz, "Deep stacked hierarchical multi-patch network for image deblurring," in *Proceedings of the IEEE/CVF Conference on Computer Vision and Pattern Recognition*, 2019, pp. 5978–5986. 4, 5
- [57] H. Chen and Z. Shi, "A spatial-temporal attention-based method and a new dataset for remote sensing image change detection," *Remote Sensing*, vol. 12, no. 10, p. 1662, 2020. 4
- [58] C. Benedek and T. Szirányi, "Change detection in optical aerial images by a multilayer conditional mixed markov model," *IEEE Transactions on Geoscience and Remote Sensing*, vol. 47, no. 10, pp. 3416–3430, 2009. 4